RESEARCH ARTICLE | JUNE 23 2025

Effects of arsenic oxides on GaAs surfaces on photoluminescence properties of buried InGaAs quantum wells: Dependence on initial surfaces before oxidation

Zhao Ma ; Takaaki Mano ; Akihiro Ohtake ; Takashi Kuroda

J. Appl. Phys. 137, 243102 (2025)
https://doi.org/10.1063/5.0274742

Journal of Applied Physics ARTICLE pubs.aip.org/aip/jap

Effects of arsenic oxides on GaAs surfaces on photoluminescence properties of buried InGaAs quantum wells: Dependence on initial surfaces before oxidation

Cite as: J. Appl. Phys. **137**, 243102 (2025); doi: 10.1063/5.0274742
Submitted: 8 April 2025 · Accepted: 29 May 2025 ·
Published Online: 23 June 2025

Zhao Ma,[1,2,a)] Takaaki Mano,[1,a)] Akihiro Ohtake,[1] and Takashi Kuroda[1,2]

AFFILIATIONS

[1]National Institute for Materials Science, Research Center for Electronic and Optical Materials, Tsukuba, Ibaraki 305-0044, Japan
[2]Department of Applied Chemistry, Graduate School of Engineering, Kyushu University, Fukuoka 819-0395, Japan

[a)]**Authors to whom correspondence should be addressed:** MA.Zhao@nims.go.jp and MANO.Takaaki@nims.go.jp

ABSTRACT

We have studied the oxidation states and photoluminescence (PL) properties of GaAs(100) samples that incorporated buried InGaAs quantum well (QW) structures prepared by molecular-beam epitaxy (MBE). The surfaces of the MBE-grown GaAs(100) samples were controlled so that they were either As-rich c(4 × 4)α, Ga-rich (4 × 6) or Se-terminated (2 × 1) structures prior to oxidation. We found that the As/Ga composition ratio at the initial GaAs surface strongly affects the oxidation processes and the resultant PL properties. An oxidized sample whose initial As-rich surface contains a large amount of As oxide, has a significantly lower PL intensity than As-deficient samples. The reduction of the surface As coverage simply by preparing Ga-rich (4 × 6) and Se-terminated (2 × 1) surfaces has a positive effect on the PL properties, which is maintained even after the oxidation has progressed into deeper layers after longer air exposure, e.g., six months.

I. INTRODUCTION

When III–V semiconductor structures are exposed to air, their surfaces are gradually oxidized by the oxygen gas and/or water vapor in the air.[1–3] It is well known that the surface oxides create a high density of surface states, which has several negative impacts on their properties, such as non-radiative recombination, Fermi-level pinning effects, and charge trapping.[4–9] The surface oxidation of III–V semiconductors has been a long-standing issue as regards improving the optical and/or electrical properties of III–V-based devices.

Recent advanced nanotechnologies allow us to fabricate highly complex nanostructures, such as nanowires, nanopillars, nanoholes, and nanodots.[10–18] With these nanostructures, the surface-related issues are more critical due to their large surface area and/or the short distance between the core region and the oxidized surfaces. In addition, it has also been suggested that the photonic properties of the nanostructures are highly sensitive to the fluctuation of the trapped charges caused by the surface states[8,9,19,20] Consequently, research on III–V semiconductor surfaces that have been exposed to the air is again attracting great attention.

One of the most promising ways of dealing with these oxide-related issues is surface termination using group-VI atoms such as sulfur (S) and selenium (Se).[21–32] It is generally believed that VI-terminated surfaces are more stable against oxidation than non-passivated III–V surfaces.[26,33,34] Recently, we have studied the effect of the S-termination of GaAs (100) surfaces on the photoluminescence (PL) properties of buried InGaAs quantum wells (QW).[35] We found that wet-chemical treatment using ammonium sulfide solution is effective in suppressing the formation of As oxide and that the PL properties are improved as the amount of As oxide is reduced. An important implication of the results is that the formation of As oxide could be suppressed by simply reducing the amount of As oxide in the GaAs sample, resulting in improved PL properties.

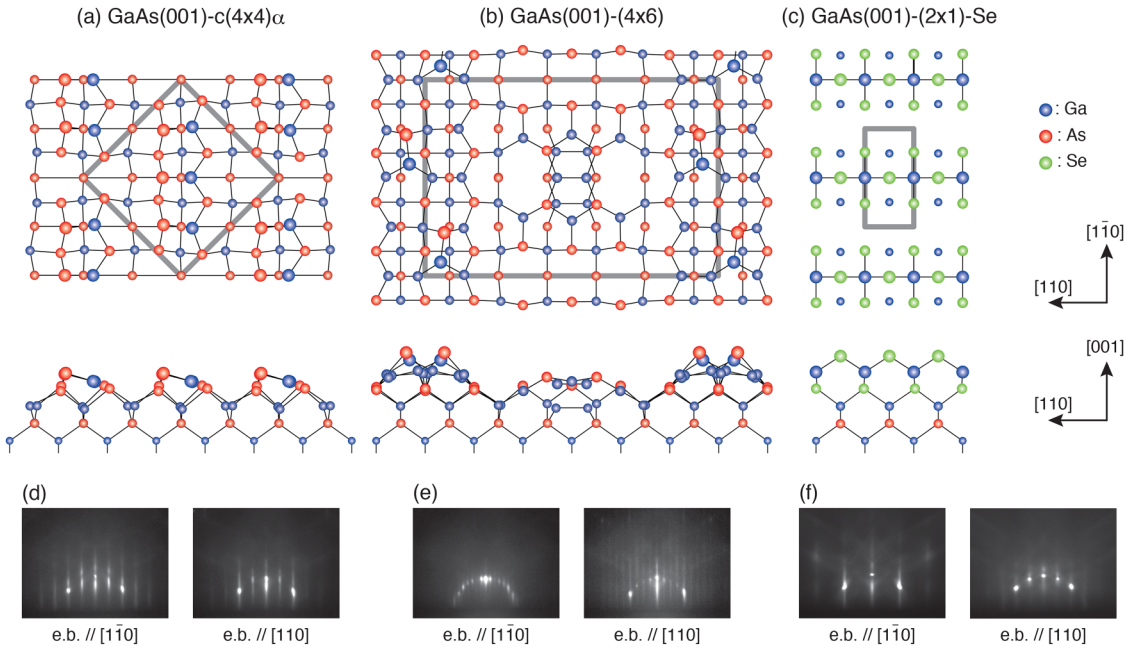

FIG. 1. (a)–(c) Structure models for GaAs (001)-c(4 × 4)α, (4 × 6), and (2 × 1)-Se surfaces. The unit cells are indicated by rectangles. (d)–(f) RHEED pattens of these surfaces obtained in the [110] and [1–10] directions. These sample surfaces were prepared by MBE.

In this study, we report on the effect of the As/Ga surface stoichiometry on oxide formation and the resultant PL properties. For this purpose, we prepared GaAs (100) samples with clean and well-defined surfaces and buried InGaAs QWs using molecular beam epitaxy (MBE) We then studied the long-term changes in the PL properties of QWs upon oxidation. A GaAs(100) surface is known to exhibit various reconstructed structures depending on the surface stoichiometry;[36] As-rich c(4 × 4)α [Fig. 1(a)][37] and Ga-rich (4 × 6) [Fig. 1(b)][38] surfaces were chosen for this study. In addition, we prepared a (2 × 1) surface terminated with Se,[32] with no As atoms in the four surface layers, as shown in Fig. 1(c). Precise control of the structure and stoichiometry of the surfaces enables us to study the effects of the surface stoichiometry on the oxide formation and the resultant PL properties. Using x-ray photoemission spectroscopy (XPS), we show that more (less) Ga oxide (As oxide) is formed on Ga-rich (As-rich) surfaces, and that samples containing more As oxide exhibit degraded PL properties. We reveal that controlling the surface so that it is Ga-rich (As deficient) is effective for enhancing the optical properties of the buried structures.

II. EXPERIMENTAL

We employed two standard MBE systems, each serving different purposes. The first MBE system was used to grow our QW samples, as well as to prepare As-rich and Ga-rich surfaces. The second MBE chamber was just used for the Se treatment. As a starting material, we prepared a single InGaAs QW structure grown on a GaAs (001) substrate using the first MBE system. A 300 nm-thick GaAs buffer layer was grown at 580 °C on a thermally cleaned substrate. Then, a 10 nm $In_{0.12}Ga_{0.88}As$ QW was grown at 490 °C, followed by a 100 nm GaAs capping layer grown at the same temperature. To suppress unintentional oxidation during the latter procedure, the sample prepared in the first MBE chamber was covered with amorphous As layers before removal. The amorphous As layers were formed by supplying As_2 flux (1×10^{-5} Torr beam equivalent pressure (BEP)) for 30 min at room temperature. The sample was then divided into several pieces. Two pieces were reloaded into the first MBE chamber for the formation of As-rich c(4 × 4)α and Ga-rich (4 × 6) reconstructions.[38,39] A Ga-rich (4 × 6) surface was prepared by heating the sample at around 540 °C without As4 flux for 5 min. To form an As-rich c(4 × 4)α surface, the sample was heated at around 540 °C under the As4 flux (BEP = 5×10^{-6} Torr) and cooled to 350 °C under the As_4 flux. Another piece of the sample was placed in the second MBE system for the Se treatment: the sample was first heated at around 540 °C under As_4 flux to remove the amorphous As layers and to form an As-rich (2 × 4) reconstruction. Then the (2 × 4) sample was further heated to 600 °C under the Se flux (without As_4 flux) to form a Se-terminated (2 × 1) surface. The sample was then cooled to 350 °C under the Se flux. All the samples were simultaneously removed from the MBE systems into the air.

Immediately after removing these samples into the air, we began to study the temporal variation in the intensities of the PL and XPS signals for up to 14 days of air exposure. We used the PL

measurements to evaluate the number of nonradiative recombination centers at the surfaces. The carriers photoexcited by the laser in the capping layers migrate to the surfaces with certain probabilities. When nonradiative recombination centers are formed on the surfaces, some carriers recombine nonradiatively, resulting in the degradation of the PL intensity of the QW.[35] For the PL measurements, we employed a Nd:YVO4 laser at a wavelength of 532 nm. The emitted PL signals were detected by a 30 cm spectrometer attached to a cooled charge-coupled device (CCD) camera. All the PL measurements were conducted at 4 K.

The surface chemical conditions were analyzed using an XPS system (Surface Science Instruments M-Probe). The XPS measurements were performed using monochromatic Al Kα radiation (1486.6 eV) at room temperature. Photoelectrons were detected at an angle of 35° from the surface. The As 3d and Ga 3d spectra were measured and fitted using a Voigt function with the ratio of Gaussian to Lorentzian components fixed at 2.5. Peak separations of 0.70 and 0.45 eV, respectively, were assumed for the 5/2 and 3/2 spin-orbit components of As 3d and Ga 3d. To eliminate the sensitivity differences in photoelectron detection among various elements and electron shells, the integrated measured intensities of each component (Ga-As, Ga-O, As-O, etc.) were divided by Scofiled's relative sensitivity factors, and were then normalized to the total intensity of the Ga 3d signals.[40]

III. RESULTS AND DISCUSSION

Figures 1(d)–1(f) show typical reflection high-energy electron diffraction (RHEED) patterns of the As-rich c(4 × 4)α, Ga-rich (4 × 6), and Se-terminated (2 × 1) surfaces prepared in our MBE systems. The well-defined and sharp patterns indicate the formation of flat, large terraces, which is characteristic of samples prepared by MBE. The proposed structural models for these surfaces are shown in Figs. 1(a)–1(c).[32,38,39] The As-rich c(4 × 4)α reconstructed surface consists of three Ga-As dimers per unit cell on the As-terminated surface (As coverage is 1.0 Ml), while there is a very small quantity of As atoms on the Ga-rich (4 × 6) surface: the As-coverage is only 1/12 Ml. In the Se-terminated sample, the amount of As at the surface layers is further reduced; Se atoms completely replace As atoms in the 1st and 2nd layers. As we report below, the three samples exhibit altogether different PL properties after being exposed to air.

In this work, we mainly analyze the low-temperature PL properties at 4 K, since the PL at higher temperatures could suffer from complicated dynamics, such as carrier thermal escape from the QW and enhancement of nonradiative recombination. Figures 2(a)–2(c) show the low-temperature PL spectra for the three samples, which were measured immediately after the samples had been removed into the air (within 30 min). All the samples exhibit a distinct PL emission peak around 860 nm from the

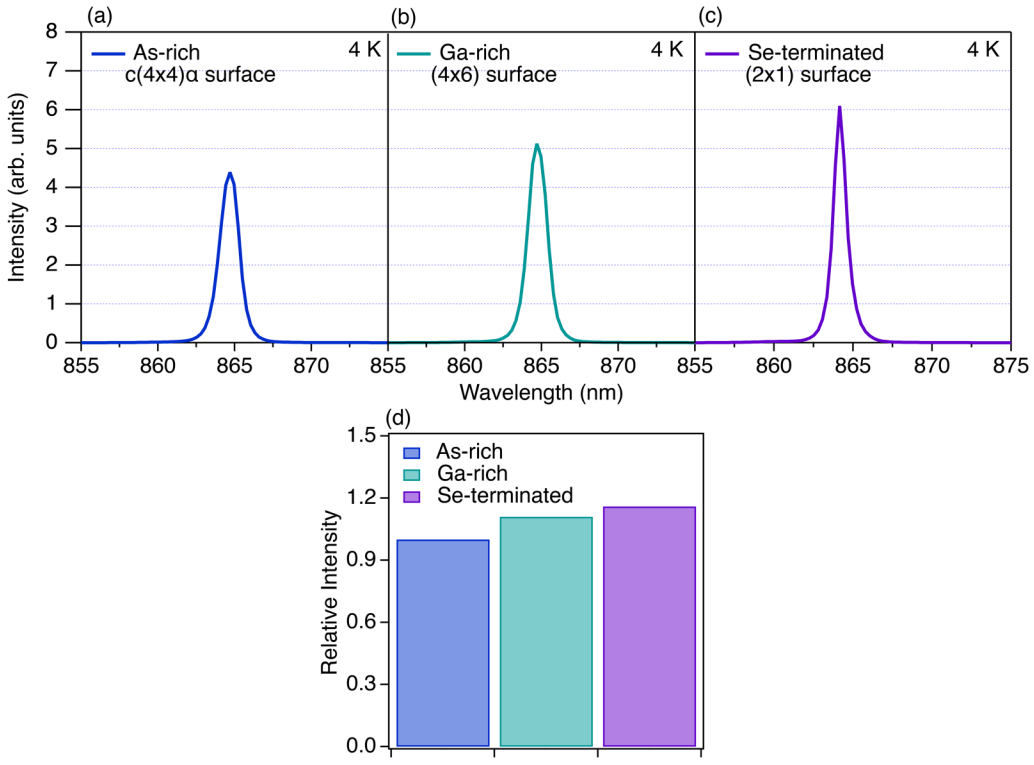

FIG. 2. Low-temperature PL spectra of (a) As-rich c(4 × 4)α, (b) Ga-rich (4 × 6), and (c) Se-terminated (2 × 1) samples. The integrated intensities of these spectra are plotted in (d).

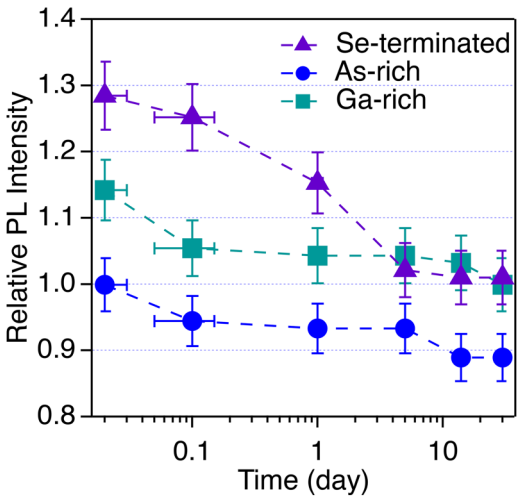

FIG. 3. Time dependent change in the integrated PL intensity of the three samples after exposure to air for a certain period of time. The measurements were made at 4 K.

InGaAs QW. The assignment of the PL spectral peak, together with other peaks, which originate from the GaAs barrier layer, was confirmed with the semilogarithmic plot shown in a (Fig. S1 in the supplementary material). There is a slight but clear difference in their intensities: the integrated PL intensities of the Ga-rich sample and Se-terminated samples were 1.11 and 1.16 times greater, respectively, than that of the As-rich sample, as shown in Fig. 2(c).

Next, we studied the temporal changes in the PL intensity of the three samples after exposure to air. Figure 3 shows the integrated PL intensities of the three samples plotted as a function of the exposure time. The Ga-rich and As-rich samples both show large decreases in their PL intensities during the first 2 h followed by gradual decreases. The degradation is attributed to the oxidation of clean GaAs surfaces, as we will show below. The PL intensities for Ga-rich and As-rich samples behave similarly as a function of the exposure time, namely they are decreased by 13% and 11%, respectively. Here, it is important to note that the As-rich sample always exhibits a lower PL intensity (~11%) than the Ga-rich sample throughout the oxidation processes. This means that the effects of the initial surface reconstruction on the PL properties are sustained for at least 30 days.

The PL intensity of the Se-terminated sample also decreased after the sample was exposed to air. However, comparing the results for samples that had no Se treatment, we found that the PL property degraded slightly more slowly, which is probably due to the suppression of oxidation by the Se termination. On the other hand, when the samples were left in air for longer, the PL intensity continuously decreased, and was finally saturated at nearly the same level as the Ga-rich sample after 5 days, but was always higher than that of the As-rich sample.

As in the practical case, we also compared the PL spectra of the three samples at room temperature after long-term air exposure in air (~6 months). Figures 4(a)–4(c) show the room temperature spectra of the samples. All samples exhibit a PL emission peak around 925 nm, which agrees with the typical room-temperature emission wavelength of the InGaAs quantum wells. The PL signals at room temperature decreased greatly compared with those measured at 4 K (not shown here) due to the carrier thermal escape from the shallow QW. Remarkably, the intensity contrast between the three samples is more significant at room temperature than at 4 K. At room temperature, the Ga-rich and Se-terminated samples show intensities twice that of the As-rich sample. We attribute the enhanced contrast to the increased probability that carriers reach the surface before being recombined in the QW. Although only photogenerated carriers generated in the upper part of the QW have a chance to reach the non-radiative recombination center at the surfaces, carriers generated in the lower part of the QW can also reach the surface due to the thermal escape. Therefore, the negative impacts could be enhanced.

We performed XPS measurements to understand the origin of the differences between the three samples qualitatively. Figure 5 shows the Ga3d- and As3d-XPS spectra of the three samples

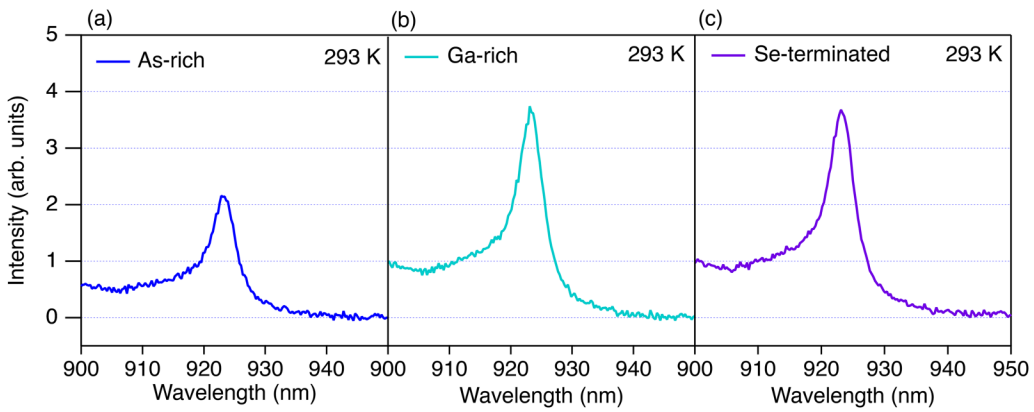

FIG. 4. PL spectra of three samples after being stored in air for 6 months. The spectra were obtained at room temperature.

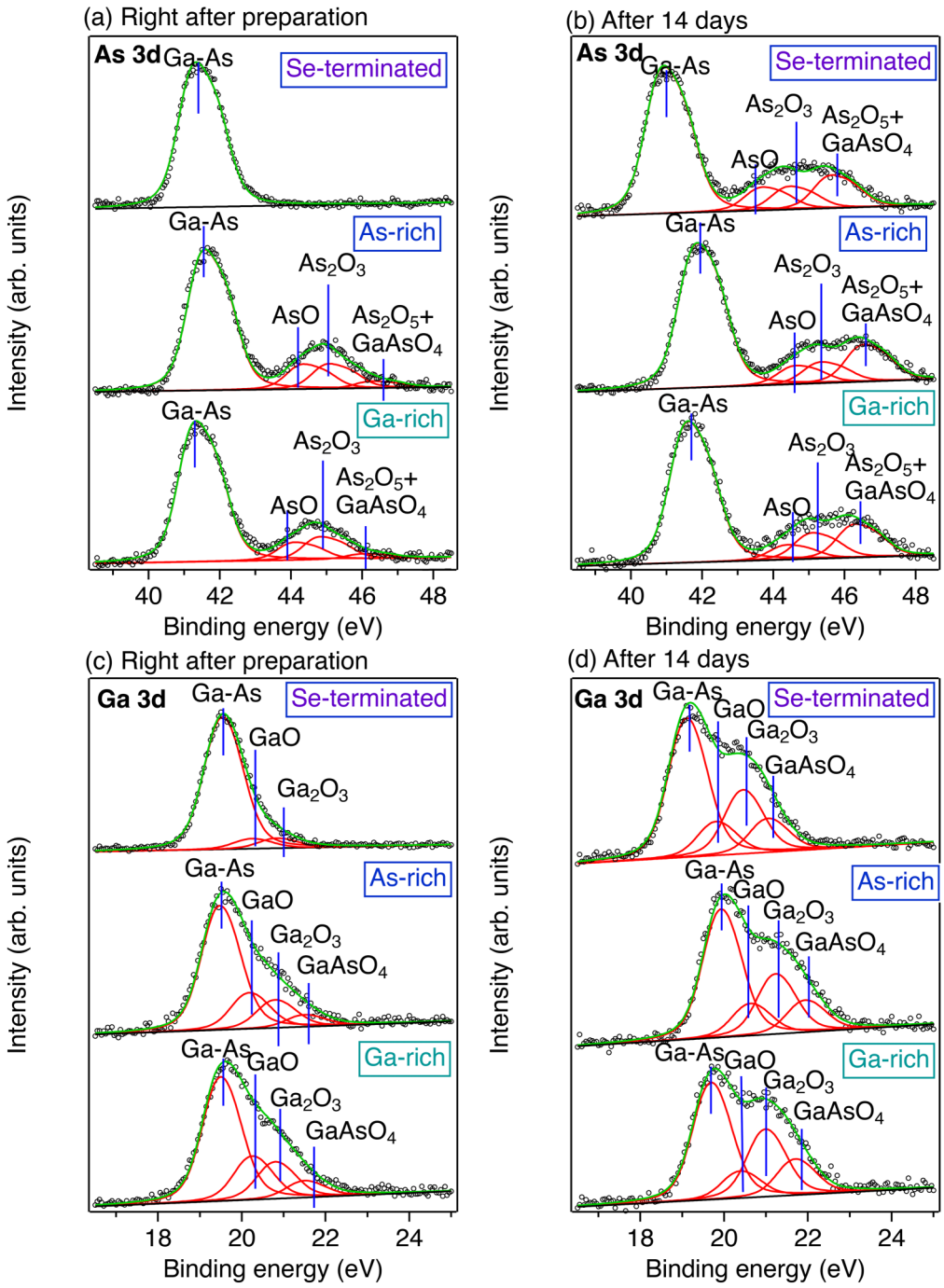

FIG. 5. As 3d and Ga 3d core-level spectra of the three samples. (a and c) right after preparation and (b and d) after exposure to air for 14 days.

immediately after preparation and after 14 days. The spectra were fitted with Ga-As and several oxide-related components. The sum intensities of the As-oxide and Ga-oxide components are plotted in Figs. 6(a) and 6(b), respectively. Just after removing the samples into the air (within 30 min), a significant amount of oxide had already formed in both the As-rich and Ga-rich samples [Figs. 5(a) and 5(c)]. As expected on the basis of the atomic structures of the initial surfaces [Figs. 1(a) and 1(b)], more As (Ga) oxide is formed

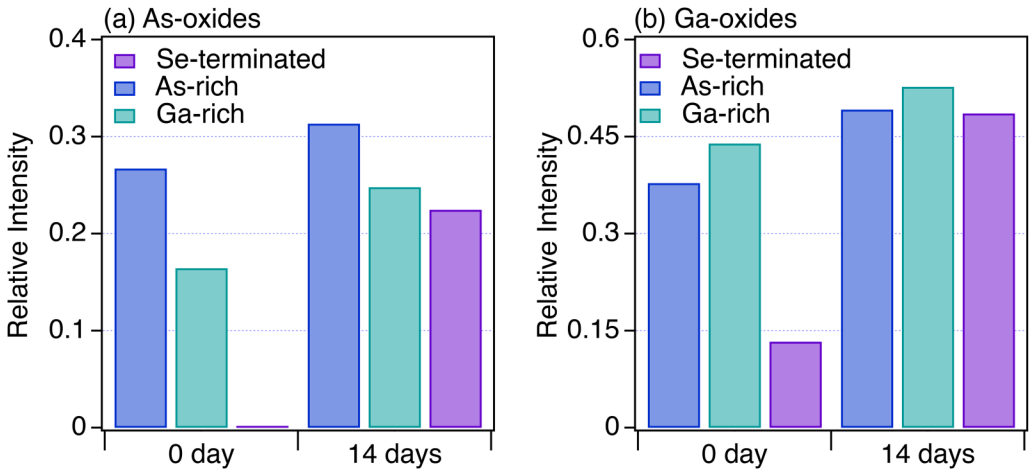

FIG. 6. The sum intensities of the (a) As-oxide and (b) Ga-oxide components of the three samples estimated from the XPS measurements. Just after removing the samples into the air (within 30 min) and after 14 days.

in the As-rich (Ga-rich) sample than in the Ga-rich (As-rich) sample, indicating that the structure and composition of the initial surfaces strongly affect the oxide formation. Since the As-rich sample exhibits weaker PL intensity, it is likely that the formation of As oxides is responsible for the degradation of the PL properties, in good agreement with our previous results for an S-terminated GaAs surface.[35]

In marked contrast with the results for As-rich and Ga-rich samples, no As-oxide components are detected in the spectrum of the Se-terminated sample measured just after preparation [Fig. 5(a), top panel]. Since, as mentioned earlier, there are no As atoms in the first four layers of the Se-terminated surface [Fig. 1(c)], it is likely that As atoms in deeper layers (>0.5 nm in depth) are not reached by the oxidation at this stage. In addition, the amount of Ga oxide is much smaller than that in the As-rich and Ga-rich samples, which is also closely related to the atomic structure of the Se-terminated (2×1) surface, in which all the Ga atoms in surface layers are fourfold-coordinated and no Ga dangling bonds are present. These results confirm that the Se-termination effectively suppresses the formation of both Ga and As oxides in the early stages of air exposure (<24 h), leading to less PL property degradation [Fig. 2(c)].

After 14 days, the amount of both the As and Ga oxides increases in all the samples, as shown in Figs. 5(b) and 5(d). In particular, the Se-terminated sample shows a more significant increase than the As- and Ga-rich samples: the amount of Ga oxide becomes almost the same as that of the other two samples and the amount of As oxide becomes almost the same as that of the Ga-rich sample. These results suggest that the effect of the Se-termination in suppressing oxide formation does not persist with longer periods of air exposure.

Since the oxidation occurs at the outermost layer of the substrate, more (less) As oxide is formed on the As-rich (As-deficient) surfaces in the initial stage of oxidation, as confirmed by XPS analysis [Figs. 5(a) and 5(c)]. Thus lower (higher) PL intensities for As-rich (As-deficient) samples (Fig. 2) indicate that As oxide at the surface has significant negative impacts on the PL properties in the early stage of oxidation. On the other hand, during a longer air exposure (>1 day), the oxidation proceeds progressively from the surface layers into deeper layers, resulting in an increase in both As and Ga oxides in all the samples, as seen in Fig. 5, which is accompanied by the degradation of the PL properties. With the Se-terminated sample, when the oxidation reaches As atoms in deeper layers (>0.5 nm deep), the As atoms begin to be oxidized, leading to a delay in the onset of the PL degradation (1 day ~ 14 days).

It has been reported that elemental As atoms are formed at the interface between oxides and GaAs substrate, which is closely related to the PL properties of GaAs.[41,42] However, since it is very difficult to detect the elemental As from an oxidized GaAs sample using XPS, we could not answer the question as to whether the possible existence of elemental As influences the PL properties of our samples. On the other hand, the present results clearly show that As oxide at the surface layers degrades the PL properties more strongly than As oxide formed in deeper layers. We conclude that preparation of an As-deficient (Ga-rich) surface structure is effective in improving the PL properties of a GaAs sample.

IV. SUMMARY AND CONCLUSIONS

We investigated the PL properties of MBE-grown GaAs/InGaAs/GaAs(100) QW structures during oxidation under atmospheric conditions. The PL properties and the oxidation processes strongly depend on the composition of the initial GaAs(100) surfaces: larger amounts of As oxide are formed in a sample with an As-rich surface of $c(4 \times 4)\alpha$, giving rise to a significant decrease in the PL intensity. On the other hand, samples with a Ga-rich (4×6) surface exhibit higher PL intensities, which could be ascribed to a lesser amount of As oxide. While Se treatment is effective in delaying the onset of the oxidation and the resultant PL degradation, no significant difference from the Ga-rich (4×6) sample was observed after 5 days exposure to air. We found that the simple preparation

of As-deficient GaAs surfaces is effective in suppressing the degradation of the PL properties of buried QW structures even after long-term atmospheric exposure.

SUPPLEMENTARY MATERIAL

See the supplementary material for an additional figure of the low-temperature PL spectrum with a logarithmic intensity scale, where each emission peak is identified.

ACKNOWLEDGMENTS

This work was supported by the Innovative Science and Technology Initiative for Security, Grant No. JPJ004596, ATLA, Japan.

AUTHOR DECLARATIONS

Conflict of Interest

The authors have no conflicts to disclose.

Author Contributions

Zhao Ma: Conceptualization (equal); Data curation (equal); Investigation (equal); Methodology (equal); Validation (equal); Writing – original draft (equal); Writing – review & editing (equal). **Takaaki Mano:** Conceptualization (equal); Funding acquisition (equal); Methodology (equal); Project administration (equal); Resources (equal); Supervision (equal); Writing – review & editing (equal). **Akihiro Ohtake:** Conceptualization (equal); Data curation (equal); Investigation (equal); Resources (equal); Supervision (equal); Validation (equal); Writing – review & editing (equal). **Takashi Kuroda:** Conceptualization (equal); Funding acquisition (equal); Project administration (equal); Resources (equal); Supervision (equal); Writing – review & editing (equal).

DATA AVAILABILITY

The data that support the findings of this study are available from the corresponding authors upon reasonable request.

REFERENCES

[1]F. Lukeš, Surf. Sci. **30**, 91 (1972).
[2]W. E. Spicer, I. Lindau, P. E. Gregory, C. M. Garner, P. Pianetta, and P. W. Chye, J. Vac. Sci. Technol. **13**, 780 (1976).
[3]M. Scarrozza, G. Pourtois, M. Houssa, M. Heyns, and A. Stesmans, Phys. Rev. B **85**, 195307 (2012).
[4]W. E. Spicer, P. W. Chye, P. R. Skeath, C. Y. Su, and I. Lindau, J. Vac. Sci. Technol. **16**, 1422 (1979).
[5]C. L. Hinkle, M. Milojevic, B. Brennan, A. M. Sonnet, F. S. Aguirre-Tostado, G. J. Hughes, E. M. Vogel, and R. M. Wallace, Appl. Phys. Lett. **94**, 162101 (2009).
[6]X. Yin, H.-M. Chen, F. H. Pollak, Y. Chan, P. A. Montano, P. D. Kirchner, G. D. Pettit, and J. M. Woodall, J. Vac. Sci. Technol. A **10**, 131 (1992).
[7]S. L. Chen, E. M. Chen, F. Ishikawa, and I. A. Buyanova, Sci. Rep. **5**, 11653 (2015).
[8]M. Hauck, F. Seilmeier, S. E. Beavan, A. Badolato, P. M. Petroff, and A. Högele, Phys. Rev. B **90**, 235306 (2014).
[9]C. F. Wang, A. Badolato, I. Wilson-Rae, P. M. Petroff, E. Hu, J. Urayama, and A. Imamoğlu, Appl. Phys. Lett. **85**, 3423 (2004).
[10]O. Demichel, M. Heiss, J. Bleuse, H. Mariette, and A. Fontcuberta i Morral, Appl. Phys. Lett. **97**, 201907 (2010).
[11]S. Manna, H. Huang, S. F. C. da Silva, C. Schimpf, M. B. Rota, B. Lehner, M. Reindl, R. Trotta, and A. Rastelli, Appl. Surf. Sci. **532**, 147360 (2020).
[12]A. Higuera-Rodriguez, B. Romeira, S. Birindelli, L. E. Black, E. Smalbrugge, P. J. Van Veldhoven, W. M. M. Kessels, M. K. Smit, and A. Fiore, Nano Lett. **17**, 2627 (2017).
[13]D. Ren, K. M. Azizur-Rahman, Z. Rong, B. C. Juang, S. Somasundaram, M. Shahili, A. C. Farrell, B. S. Williams, and D. L. Huffaker, Nano Lett. **19**, 2793 (2019).
[14]B. Jacob, F. Camarneiro, J. Borme, O. Bondarchuk, J. B. Nieder, and B. Romeira, ACS Appl. Electron. Mater. **4**, 3399 (2022).
[15]H. Q. T. Bui, R. T. Velpula, B. Jian, M. R. Philip, H. D. Tong, T. R. Lenka, and H. P. T. Nguyen, Appl. Opt. **59**, 7352 (2020).
[16]A. Lin, B. L. Liang, V. G. Dorogan, Y. I. Mazur, G. G. Tarasov, G. J. Salamo, and D. L. Huffaker, Nanotechnology **24**, 075701 (2013).
[17]X. Cao, J. Yang, P. Li, Y. Zhang, E. P. Rugeramigabo, B. Brechtken, R. J. Haug, M. Zopf, and F. Ding, Appl. Phys. Lett. **118**, 221107 (2021).
[18]M. Hartensveld, G. Ouin, C. Liu, and J. Zhang, J. Appl. Phys. **126**, 183102 (2019).
[19]A. Berthelot, I. Favero, G. Cassabois, C. Voisin, C. Delalande, P. Roussignol, R. Ferreira, and J. M. Gérard, Nat. Phys. **2**, 759 (2006).
[20]N. Ha, T. Mano, Y. L. Chou, Y. N. Wu, S. J. Cheng, J. Bocquel, P. M. Koenraad, A. Ohtake, Y. Sakuma, K. Sakoda, and T. Kuroda, Phys. Rev. B **92**, 075306 (2015).
[21]C. J. Sandroff, R. N. Nottenburg, J. C. Bischoff, and R. Bhat, Appl. Phys. Lett. **51**, 33 (1987).
[22]M. S. Carpenter, M. R. Melloch, M. S. Lundstrom, and S. P. Tobin, Appl. Phys. Lett. **52**, 2157 (1988).
[23]J. F. Fan, H. Oigawa, and Y. Nannichi, Jpn. J. Appl. Phys. **27**, L1331 (1988).
[24]Y. Nannichi, J. F. Fan, H. Oigawa, and A. Koma, Jpn. J. Appl. Phys. **27**, L2367 (1988).
[25]C. J. Sandroff, M. S. Hegde, L. A. Farrow, R. Bhat, J. P. Harbison, and C. C. Chang, J. Appl. Phys. **67**, 586 (1990).
[26]M. Oshima, T. Scimeca, Y. Watanabe, H. Oigawa, and Y. Nannichi, Jpn. J. Appl. Phys. **32**, 518 (1993).
[27]H. Oigawa, J.-F. Fan, Y. Nannichi, K. Ando, K. Saiki, and A. Koma, Jpn. J. Appl. Phys. **28**, L340 (1989).
[28]H. Oigawa, J. F. Fan, Y. Nannichi, H. Sugahara, and M. Oshima, Jpn. J. Appl. Phys. **30**, L322 (1991).
[29]T. H. Yu, L. Yan, W. You, R. B. Laghumavarapu, D. Huffaker, and C. Ratsch, Appl. Phys. Lett. **103**, 173902 (2013).
[30]H. Xu, S. Belkouch, C. Aktik, and W. Rasmussen, Appl. Phys. Lett. **66**, 2125 (1995).
[31]S. Tsukamoto and N. Koguchi, Appl. Phys. Lett. **65**, 2199 (1994).
[32]A. Ohtake, T. Suga, S. Goto, D. Nakagawa, and J. Nakamura, Sci. Rep. **13**, 18140 (2023).
[33]R. Richter and H. L. Hartnagel, J. Electrochem. Soc. **137**, 2879 (1990).
[34]T. Scimeca, Y. Watanabe, F. Maeda, R. Berrigan, and M. Oshima, J. Vac. Sci. Technol. B **12**, 3090 (1994).
[35]Z. Ma, T. Mano, A. Ohtake, and T. Kuroda, Jpn. J. Appl. Phys. **63**, 121002 (2024).
[36]A. Ohtake, Surf. Sci. Rep. **63**, 295 (2008).
[37]A. Ohtake, J. Nakamura, S. Tsukamoto, N. Koguchi, and A. Natori, Phys. Rev. Lett. **89**, 206102 (2002).
[38]A. Ohtake, P. Kocán, J. Nakamura, A. Natori, and N. Koguchi, Phys. Rev. Lett. **92**, 236105 (2004).
[39]A. Ohtake, P. Kocán, K. Seino, W. G. Schmidt, and N. Koguchi, Phys. Rev. Lett. **93**, 266101 (2004).
[40]M. P. Seah and W. A. Dench, Surf. Interface Anal. **1**, 2 (1979).
[41]D. W. Langer, F. L. Schuermeyer, R. L. Johnson, H. P. Singh, C. W. Litton, and H. L. Hartnagel, J. Vac. Sci. Technol. **17**, 964 (1980).
[42]V. M. Mikoushkin, A. P. Solonitsyna, and E. A. Makarevskaya, Appl. Surf. Sci. **504**, 144601 (2020).